PCCP

Accepted Manuscript

ROYAL SOCIETY OF CHEMISTRY

www.rsc.org/pccp

Physical Chemistry Chemical Physics
CREATED USING THE RSC LaTeX PCCP ARTICLE TEMPLATE – SEE www.rsc.org/electronicfiles FOR DETAILS

Formation and Dynamics of "Waterproof" Photoluminescent Complexes of Rare Earth Ions in Crowded Environment†

Tetyana Ignatova,[a‡] Michael Blades,[a] Juan G. Duque,[b] Stephen K. Doorn,[c] Ivan Biaggio,[a] and Slava V. Rotkin*[d]

Received Xth XXXXXXXXXX 20XX, Accepted Xth XXXXXXXXX 20XX
First published on the web Xth XXXXXXXXXX 200X
DOI: 10.1039/b000000x

Understanding behavior of rare-earth ions (REI) in crowded environments is crucial for several nano- and biotechnological applications. Evolution of REI photoluminescence (PL) in small compartments inside a silica hydrogel, mimic to a soft matter bio-environment, has been studied and explained within a solvation model. The model uncovered the origin of high PL efficiency to be the formation of REI complexes, surrounded by bile salt (DOC) molecules. Comparative study of these REI/DOC complexes in bulk water solution and those enclosed inside the hydrogel revealed a strong correlation between an up to 5x-longer lifetime of REIs and appearance of the DOC ordered phase, further confirmed by dynamics of REI solvation shells, REI diffusion experiments and morphological characterization of microstructure of the hydrogel.

Rare Earth ions (REI) are widely used as bio-labels and dyes due to their unique photoluminescence (PL) properties.[1–6] PL lifetime is a quantity determining the REI luminescence efficiency as well as a sensitive probe for solvation state of these ions. When attached to a biomolecule REIs typically exist in the partially hydrated state, with the fully hydrated state being observed for free ions in salt solution.[7,8] PL properties of both free REIs and partially screened ions, bound to single wall carbon nanotubes (SWNT), have been studied previously in water **bulk** solution.[9–11] The behavior of a rare earth ion in a crowded environment, inside a nanoscale compartment, or in a multicomponent water solution like the intra-cellular environment, especially in the process of hydration, and PL dynamics in its transient states are of significant interest.

Monitoring the modification of terbium PL lifetime and its spectral properties in a complex environment allowed us to determine the influence of nanoscale constriction and ordered phases of surfactant molecules on the REIs and to propose a model for their solvation. The surfactant we use, sodium deoxycholate (DOC), is a bile salt, which possesses exclusive biological properties. It is known to form aggregates in water, both small (bile salt micelles) and large (tubes),[12–15] different from typical micelles formed by other surfactants. Large tubular aggregates make highly ordered phases: crystals, liquid crystals and whiskers.[15] Their phase transformations are known to be very slow and the phase equilibrium can be shifted by adding monovalent salt (NaCl and NaBr) solutions.[16] Bile salts readily form mixed micelles with both organic and inorganic substances, insoluble by themselves. For example, DOC is commonly used to dissolve SWNTs, separate SWNT fractions, and prevent reaggregation in water solution.[17–19] Lanthanide ions were shown to form complexes with bile salts[20,21] and other surfactants.[22]

As a prototype of a crowded environment we chose silica hydrogels. These hydrogels have pores with multiple scales, from nm to μm, and can be intercalated by various materials during gelation stage or after the synthesis. In this work samples ranging from silica hydrogels with SWNTs dispersed with DOC, to hydrogels with DOC, to the silica hydrogels only, as well as bulk DOC water solutions were studied. Due to the ability of SWNTs to define the structure of the immediately surrounding surfactant layer,[23] their addition as a component of the hydrogel matrix provides a route to template the local morphological structure and impact related diffusive behaviors.

As shown below Tb forms a number of complexes with DOC molecules, including in the ordered phase.The complexes manifest themselves in the steady-state and time-resolved PL spectroscopy measurements, as well as produce a characteristic microscale morphology of gel materials, observable (*ex situ*) by SEM. Evolution of these complexes in

† Electronic Supplementary Information (ESI) available: ESI provides details on Sample preparation; Photoexcitation spectrum of Tb ion; PL lifetime calculations; Spectral Distribution Functions for transient Tb states; Steady state PL data. See DOI: 10.1039/b000000x/

[a] *Physics Department, Lehigh University, 16 Memorial Drive East, Bethlehem, PA, 18020, USA.*
[b] *Los Alamos National Laboratory, Chemistry Division, C-PCS, MS J563, Los Alamos, NM 87544, USA.*
[c] *Los Alamos National Laboratory MPA-CINT, MS K771, Los Alamos, NM 87545, USA.*
[d] *Physics Department, and Center for Advanced Materials and Nanotechnology, Lehigh University, 16 Memorial Dr. E., Bethlehem, PA 18015. Fax: 1-610-758-5730; Tel: 1-610-758-3930; E-mail: rotkin@lehigh.edu*
‡Present address: Department of Physics and Astronomy, UCI, Irvine, CA.

the limited volume inside the pores of the silica hydrogel has been traced *in situ* in the course of penetration of the REIs through the hydrogel. By measuring the dynamics of complex formation and spatial correlation of the transient state during REI diffusion into a silica hydrogel and combining this with additional spectral data, a reliable model of RE photoluminescence is developed below.

Terbium (III) chloride (99.99% from Sigma Aldrich) was dissolved in deionized (DI) water.All gels were made using the standard CVD technique described in detail elsewhere.[24] During the hydrolysis of tetramethylorthosilicate the silica was produced in the form of primary particles with a size of tens of nanometers.[25] The primary particles aggregate and form secondary particles of μm size, making a gel structure with interparticle pores of various sizes, filled with water, DOC water solution, or SWNT/DOC water solution. $TbCl_3$ was carefully added during the gel synthesis in a series of the samples. All other PL samples were prepared by adding terbium chloride DI water solution (with maximum concentration of 10% w.u.) into a cuvette with the hydrogel or the DOC solution (Figure S1 in SI) and waiting until the diffusion process completed.

Time-resolved PL experiments were done using a 20 ps tunable laser source (OPG/OPA, EKSPLA model PG401) with the repetition rate of 10 Hz. PL of the $^5D_4$ state was obtained after excitation at 2.55 eV (486 nm, see Figure S2 for PL excitation profile and Figure S6, inset for Tb optical transitions). The laser beam (17.4 μJ) was focused into the center of the sample cuvette. Perpendicular to the incident beam a pair of collection lenses gathered the PL signal and focused it onto the entrance slit of a photomultiplier tube detector connected to a digital oscilloscope (Lecroy, Waverunner LT 584). Two filters: a 488 nm long pass to cut the scattered incident laser beam, and a 540$\pm$10 nm band pass to extract the $^5D_4 \rightarrow {}^7F_5$ Tb line from the total PL signal, were used. The steady-state Tb emission spectra were obtained with a Horiba JobinYvon 41000 Raman spectrometer with CW Ar laser at 488 nm of excitation.

Efficient photoluminescence of Tb was observed in all hydrogel samples (Figure 1f) despite a low absorption cross section of this RE in the visible and near-UV region. This gives an early indication of changes in the Tb solvation state. Furthermore, both the shape of steady-state PL lines and the decay time measured by time resolved PL spectroscopy vary in the hydrogel as compared to the bulk water solution where Tb exists as a fully hydrated ion. Time resolved spectroscopy of Tb^{3+} gives the lifetime varying by more than 5 times in different surroundings. Figure 1a shows time-resolved emission decay of Tb in DI water solution (blue), Tb in DOC silica hydrogel (green), and Tb in DOC/SWNT silica hydrogel (red). The curves were fitted by a monoexponential decay to extract the PL lifetimes. Similar data was collected for all samples and the results are summarized in Figure 1e and Table 1. We argue that the changes in the lifetime, which are directly related to the PL efficiency, reflect the structure of photoluminescent complexes of REI, forming in DOC solution and DOC gel (ordered phase) and further evolving in the nano-porous environment.

Indeed, the $^5D_4 \rightarrow {}^7F_5$ electronic transition at 2.27 eV (545 nm) in Tb^{3+} is a 4f$\rightarrow$4f transition. The valence 4f electrons are well shielded from the environment by the outer core 5s and 5p electrons and minimally involved in bonding. Because of this shielding, the properties of these ions are typically retained after complex formation. Despite this fact, the luminescence of solvated REIs is weak and its efficiency strongly depends on the environment due to significant nonradiative recombination through the O-H vibrations of the water molecules in the solvation shell. The method to estimate the number of water molecules in the first solvation shell by measuring PL lifetime was proposed in Ref.[11] Moreover, the spectral lines of Tb PL show characteristic broadening in water solution (see inset in Figure 1a and Figures S6-S7). It has been already shown that the addition of chelating agents and encapsulation of the REIs in chelate shells or in surfactant micelles lead to longer emission lifetimes and consequently to higher quantum yields.[26–28] Our time-resolved PL data confirm that the interaction of Tb^{3+} with DOC leads to complex formation that results in long PL decay times, at least 1.1 ms and longer, compared with Tb^{3+} in water solution: τ =0.38 ms.

More than 250% longer lifetime was observed after encapsulation of REIs in the DOC filled hydrogel. This is due to DOC molecules displacing about 7 water molecules from the REI solvation shell (Figure 1e). However, the initial change of τ can be followed by even stronger isolation of REI inside DOC gel and structural ordered phases. We observe formation of long-lived Tb complexes in all DOC samples, though placing Tb^{3+} in a crowded environment results in the largest improvement of the photoluminescence as compared to bulk water solution. A two times increase of the lifetime, corresponding to elimination of 1-2 extra water molecules from the solvation shell, happened inside the hydrogel with the time.

Analysis of the large set of PL lifetime data suggests that our samples fall into three groups, where the Tb ion exists in different solvated/encapsulated states (Figure 1e). In the type I group, which includes $TbCl_3$ water solution, Tb inside of a silica hydrogel (not containing DOC), and terbium acetate water solution, the fully solvated (hydrated) Tb ions were found with the typical lifetime τ = 0.38-0.48 ms (slightly higher for $Tb(CH_3CO_2)_3$), corresponding to 7-9 solvation water molecules. The type II materials contain Tb ions partially screened from the water due to interaction with the DOC molecules, slowly forming micelles, suspended in solution, with the characteristic lifetime increased to τ =1.1-1.5 ms. The significant increase of PL lifetime indicates the weaker interaction or smaller number of OH groups in the nearest

vicinity of the Tb ion. Following[11] we can estimate that the number of solvation water molecules decreases by 6-7 on average. The type II behavior was also seen in some gel samples in the initial stage of REI diffusion as will be explained later.

For type III even longer lifetimes (τ =1.85-2.5 ms) are achieved. The difference in the Tb lifetimes for hydrogels with and without nanotubes is reproducible and most likely is due to the sample (gel) morphology difference. Reproducibly, type III hydrogels have more stable structure, and the Tb diffusion is strongly inhibited and takes days for these samples. We speculate this may be due to DOC having already formed micelles or gel-like structures during the synthesis. This conclusion is supported by the measured Tb diffusion coefficient (lower than $10^2\ \mu m^2/s$) to be discussed elsewhere[29,30]. In type III materials the long-lived state corresponds to the Tb/DOC complexes packed in the pores of the hydrogel. We note that one can reject the model of interaction of pure Tb ions with the silica or SWNT (not involving DOC) because of the different Tb behavior in DOC gel and bulk DOC solution samples vs. samples without bile salt (gel and solution). We emphasize the strong correlation of both the lifetime and the peak shape of steady-state PL in the presence or absence of DOC (Figure 1a). Thus the DOC-REI interaction and the *structure* of the DOC ordered phase are critical to explain the physics of observed phenomena.

We followed the evolution of the solvation state during diffusion of Tb^{3+} ions through the DOC/SWNT hydrogel. Figure 2a presents the linear-log plot of the PL decay signal for Tb taken near the top of the sample (location indicated by dark blue arrow in Figure 3a, inset) with different delay times, 10 to 56 min, after $TbCl_3$ DI water solution was added at the top of the hydrogel. The PL signal at $t < 10$ min was not useful due to a low signal-to-noise ratio corresponding to a vanishing concentration of REI, not penetrated in the sample yet. The curves show evolution of the Tb PL in the course of slow diffusion. The decay has a stretched exponential form (note linear-log scale of the plot) and is characterized by more than one lifetime. In order to clarify the nature of this non-mono-exponential decay we performed spectral analysis of the PL signal, similar to one suggested in earlier works[31,32]. The PL data was fit by:

$$I(t) = \int g(\tau) e^{-t/\tau} d\tau \qquad (1)$$

where $g(\tau)$ represents a spectral distribution function (SDF) and, as we show next, is characteristic of the sample. Similar analysis has been performed on other PL data: for example, on Figure 1b the typical SDF of Tb water solution is presented which shows a single, very sharp ($\pm$0.01 ms, compare the inset) peak around 0.40 ms, the lifetime of a fully solvated Tb ion, as well as two typical SDF spectra of Tb in DOC/SWNT hydrogel samples, with the single lifetime longer than 2 ms, although broader in Sample 1 due to experimental time resolution. This SDF data is consistent with the excellent mono-exponential fit of Figure 1a. We note that such samples need to be "aged" for days to weeks, depending on the hydrogel morphology. We propose that the mono-exponential decay of long-lifetime samples is due to the highest order of the DOC phase, where REIs are incorporated in crystallographic positions. Ref.[33] presents a similar model for alkaline ions inside the DOC tubular phase. In such a structure the number of water molecules, co-crystallized with the REI, is fixed and small. This results in single value for the lifetime, much longer than in bulk water. Less ordered samples, including DOC-micellar phase in DOC bulk solutions, show multiple times corresponding to multiple Tb locations. With time such phases may also transform into the equilibrium highly ordered structure, thus increasing the τ, though it may take weeks as in our experiments due to a slow phase transition. Such slow dynamics of the DOC phase transformation was also observed in Refs.[34–36]. Next we present data on photoluminescence of REI in both the final products and the transient states.

SDF plots of Tb PL during the early stages of diffusion (delay time less than an hour) presented in Figure 2b show a clear bi-exponential distribution (except for the red curve at $t = 10$ min where the signal is still too weak due to small amount of diffused Tb). The long-lived complex formed by REI immediately upon mixing with DOC in the crowded environment of the type II silica hydrogel has the lifetime τ_2 =1-1.5 ms which is lower than the lifetime observed in the bulk DOC solution after it reached its steady state. Thus one should attribute this peak to the transient state. An interesting question about existence of transient Tb states in bulk DOC solution may deserve special study. Increasing average value of τ_2 gives us evidence that Tb ions form highly photoluminescent complexes with DOC while penetrating into the hydrogel. Comparing radiative and nonradiative lifetimes for different Tb spectral lines (see Fig. 1c and S8 and also discussion after Eq.(3)) we conclude that this is due to suppression of the nonradiative recombination channel into the water vibration modes. REIs in these transient states are better screened from water molecules, although not as well as in the completely ordered DOC phase (Figure 1a). We suggest that REIs form bonds with bile salt molecules and this triggers their gelation in both bulk water solution and porous hydrogel matrix which contains DOC. This process is clearly seen by the color of the sample changing upon adding Tb: the samples become "milky" due to larger light scattering by micelles/complexes or phase boundaries (Figure 1f and S1). Morphology of these sub-micrometer structures can be visualized by SEM on the dried gel samples (Figure 3c).

On the contrary, well formed DOC (gel) structures existed even before adding Tb solution in a different set of hydrogel samples (type III), which was clearly recognized by hindered Tb diffusion with typical propagation rates of cm/days. These

samples always show singular, large values of τ_2 =2.1-2.3 ms. The type II hydrogel samples typically take weeks to months to reach such ordered state.

We turn now to the short lifetime, $\tau_1 \simeq$0.45 ms, which is close to the lifetime of fully solvated ion in $TbCl_3$ DI water solution (Figure 1a,b). This transient state is clearly observed after a delay on the order of the diffusion time, estimated to be 10 min (for 0.5 mm distance). The corresponding short-lived state shows little variation of lifetime during further diffusion processes, while the long-lived state has gradually increasing lifetime, becoming more and more stable against non-radiative recombination by water. This is further evident when all transient SDF data is compared with Tb in pure water and in "aged" hydrogel samples (initial and final products), as shown in the 3D plot in Figure 2c. The type III hydrogels were added to the plot for comparison, where the ordered DOC phase existed before adding RE and no Tb state with a short lifetime was observed at all. An arrow indicates evolution of the long-lived Tb state, born in the early stage of diffusion into DOC inside the hydrogel, developing into the complete bile salt complexes/micelles more that 3 weeks later. We emphasize that, although the transient short-lived state is still dominant at $t = 56$ min delay, it almost totally disappears after the long period of aging of the sample (Figure 1a and 1b). We speculate that the transient state may correspond to the Tb partially coordinated between DOC molecules, making an initial DOC-gel structure, solvated by larger number of water molecules. With time, bigger DOC (tubular) aggregates or other DOC high order phases[15,35] start to grow. REIs slowly penetrate in aggregates, expelling excess water outside, and forming the steady-state long-lived "water-proof" complexes inside. The morphological features associated with such structures were observed in high-resolution SEM of samples prepared from both DOC solution and silica hydrogel. Figure 3c shows large field of view images of the gel residue (from DOC solution) and Figure 3d shows hydrogel collected on a TEM grid, while insets emphasize close similarity of the porous and multiconnected complexes in both samples (note 10× decrease of the scale bar in consequent inset images), although the pore size for the DOC/SWNT hydrogels is somewhat smaller and the structure is less open than that for gels based solely on DOC. Such morphological differences are consistent with the decreased diffusion rate and increased REI photoluminescence lifetimes found in the DOC/SWNT gels.

Given the SDF is strongly peaked at 2 values, we fit the PL data on Figure 2a by bi-exponential decay:

$$I(t) = i_o + A_1 e^{-t/\tau_1} + A_2 e^{-t/\tau_2} \qquad (2)$$

where the background level, i_0, is set by the zero level reached by the PL signal several milliseconds after excitation, when it becomes indistinguishable from background noise. Resulting amplitudes (A_1 and A_2) and lifetimes (τ_1 and τ_2) are plotted vs. diffusion time in Figure 2d. The concentration of the short-lived state (blue) first increases abruptly when the diffusion process reached the observation point (indicated by the upper arrow in Figure 3a inset). Then it steadily grows which corresponds to continuing diffusion of Tb inside the sample. Although the long-lived state (red) forms immediately upon mixing REI solution with the DOC, its lifetime increases with diffusion, due to evolution of the DOC gel and Tb complexes inside. After several weeks REIs will create the long-lived complexes with DOC with $\tau_2 \simeq$2 ms, given the REI amount is not in excess (Figure 1c). In type II samples we still observed the short-lived state of Tb after aging, although in low-trace amounts. This strongly correlates with the type II hydrogel morphology, being less stiff before adding Tb (no DOC gel formed yet) and showing faster Tb diffusion, possibly due to larger pore size and water content.

After 80 min of diffusion of REI in the type II hydrogel we measured the spatial distribution of Tb in its transient DOC complexes ($\tau_2 >$1 ms) and in the states accessed by water ($\tau_1 <$0.5 ms). The results are presented in Figure 3a with the color code (blue-cyan-pink-brown) showing the depth of the observation location (top-to-bottom).The SDF becomes broader with the depth (as shown in Figure S5 in SI) and it further shifts toward long lifetime, same as in ordered DOC phase. A bi-exponential fit reveals the relative concentration of hydrated Tb and transient Tb-DOC complexes as a function of the diffusion depth (Figure 3b). Significant amounts of Tb ions exist in the long-lived, "water-resistant" complexes even at the bottom part of the sample. Formation of such complexes happens "instanteneously", at least much faster than the diffusion of the hydrated ions (maximum diffusion depth can be estimated as ∼1-2 mm in 80 min). In fact, it already happened deep inside the sample at the smallest (10 min) delay, as confirmed by Figure 2. This behavior deserves further study to be presented elsewhere[29,30]. Obviously REI cannot reach the bottom of the sample by mere diffusion during the delay time of experiment. Even so, the concentration for both types is non-zero everywhere inside the sample, as shown on the top panel of Figure 3b. Relative abundance of hydrated ions is considerably higher at the top of the tube due to continuing diffusion of REI from the top solution. The diffusion is slowed down at the phase boundary, clearly visible in the optical image in Figure 3a, inset (near purple arrow), as well as in Figure 3b as a kink of the blue curve. We observed that until this boundary crosses the whole sample the formation of long-lived complexes is hindered in the bottom phase. Even after the boundary passed, the material is still "aging" and the steady state is not reached yet. Most likely, a higher concentration of REI is needed to initiate the formation of final, high order DOC phases and the transformation of the transient complexes. This correlates with the role played by other salts in stabilizing the DOC gelation. Recent work[16] showed

that monovalent sodium salts can shift the equilibrium towards DOC agglomeration, which suggests that the effect of multivalent REIs should be even stronger. An average Tb concentration in our samples can be estimated as 10-30 mM.

The steady-state PL spectroscopy measurements demonstrate the expected increase of the emission signal (inset in Figure 1a) in Tb/DOC solution and even more in Tb/DOC/SWNT hydrogel. The PL Quantum Yield (QY), proportional to the non-radiative lifetime:

$$QY = \frac{\tau_{nrad}}{\tau_{rad} + \tau_{nrad}} \simeq \frac{\tau_{nrad}}{\tau_{rad}} \quad (3)$$

increases from 1.3% in the Tb water solution[9] to 6.4% in Tb/DOC/SWNT hydrogel and 4.9% in Tb/DOC bulk solution. We note that if the radiative rate $1/\tau_{rad}$ would change, for example, due to change in the "crystal" field of the environment around the REI,[28,37] the relative oscillator strengths of $^5D_4 \rightarrow {}^7F_j$ transitions should vary. The partial QY for the 4 lowest optical transitions (symbols) during the formation of complexes with DOC is shown in Figure S8 along with the theoretical fit (solid curves) based on Eq.(3). For the concentration of DOC added to $TbCl_3$ solution up to 75 mM no significant dependence was observed, thus we assume τ_{rad} to be the same in all samples (though different for each ^7F_j transition). On contrary, Fig. 1c shows that the non-radiative rate is the same for different ^7F_j transitions (of the same sample).

In conclusion, we studied the behavior of Tb ions in different environments. We found that Tb ions form long-lived PL complexes in solution containing surfactant (DOC) molecules. Tb ions form similar complexes in silica hydrogels containing DOC. The process of forming transient complexes is faster than the diffusion through the DOC water solution or DOC/SWNT silica hydrogel. Upon penetration of Tb in the ordered DOC phase the PL lifetime in these "water-proof" complexes increases up to 2.3 ms for DOC/SWNT hydrogel, although the dynamics of Tb in DOC phase is very slow (fully develop in hours to weeks), similar to dynamics of phase transformation in pure DOC. Close similarity of the shape of Tb lines of steady-state PL spectra in DOC bulk solution and DOC/SWNT silica gel, contrasted to $TbCl_3$ water solution, suggests the formation of DOC micelles and then DOC ordered phases in both cases, further supported by their similar morphology as detected by SEM. An additional increase of PL signal (and lifetime), reproducibly observed upon delayed diffusion of REIs in or between the DOC micelles/complexes inside the crowded environment of the hydrogel, should be due to decreasing number of water molecules in REI solvation shells in a densely packed DOC ordered phase. Such a phase should form readily inside the pores between the silica particles. The process is stabilized by a high concentration of multivalent REIs. The general increase of Tb lifetime in gels also containing SWNTs is suggestive of a special role such one-dimensional objects may play in templating surfactant structures within the silica gel which will be the subject of a more detailed follow-on study. The soluble REI complexes with strong and water stable PL can be useful for biophysical imaging of REIs in cells and tissues. Understanding the dynamic behavior of transient states of REI in various surroundings is important for quantitative analysis of microscopy and spectroscopy data.

Acknowledgements: This work was performed in part at the Center for Integrated Nanotechnologies, a U.S. Department of Energy, Office of Basic Energy Sciences user facility (User Grant C2011B77); TI and SVR acknowledge support of NSF (ECCS-1202398); JGD thanks the DOE-LDRD Early Career fellowship.

Table 1 Tb^{3+} PL lifetime of $^5D_4 \rightarrow {}^7F_5$ transition in various environment

	Long lifetime, ms	Short lifetime,ms
DI water solution	–	0.380±0.005
silica hydrogel	–	0.380±0.005
Tb acetate water solution	–	0.480±0.005
DOC DI water solution	1.50±0.02	0.40±0.02
DOC silica hydrogel	1.85±0.02	0.40±0.02
DOC/NT silica hydrogel	2.10-2.30±0.02	0.40±0.02

References

1 J. H. Choi, A. S. Banks, T. M. Kamenecka, S. A. Busby, M. J. Chalmers, N. Kumar, D. S. Kuruvilla, Y. Shin, Y. He, J. B. Bruning, D. P. Marciano, M. D. Cameron, D. Laznik, M. J. Jurczak, S. C. Schurer, D. Vidovic, G. I. Shulman, B. M. Spiegelman and P. R. Griffin, *Nature*, 2011, **477**, 477–481.

2 B. K. Gupta, P. Thanikaivelan, T. N. Narayanan, L. Song, W. Gao, T. Hayashi, A. Leela Mohana Reddy, A. Saha, V. Shanker, M. Endo, M. A. A. and P. M. Ajayan, *Nano Letters*, 2011, **11**, 5227–5233.

3 D. J. Posson, P. Ge, C. Miller, F. Bezanilla and P. R. Selvin, *Nature*, 2005, **436**, 848–851.

4 D. L. Rosen, C. Sharpless and L. B. McGown, *Analytical Chemistry*, 1997, **69**, 1082–1085.

5 D. Jin and J. A. Piper, *Analytical Chemistry*, 2011, **83**, 2294–2300.

6 S. M. Riddle, K. L. Vedvik, G. T. Hanson and K. W. Vogel, *Analytical Biochemistry*, 2006, **356**, 108 – 116.

7 N. G. Walter, N. Yang and J. M. Burke, *Journal of Molecular Biology*, 2000, **298**, 539 – 555.

8 F. S. Richardson, *Chemical Reviews*, 1982, **82**, 541–552.

9 T. Ignatova, H. Najafov, A. Ryasnyanskiy, I. Biaggio, M. Zheng and S. V. Rotkin, *ACS Nano*, 2011, **5**, 6052–6059.

10 P. K. Avti and B. Sitharaman, *International Journal of Nanomedicine*, 2012, **7**, 1953–1964.

11 W. D. Horrocks and D. R. Sudnick, *Accounts of Chemical Research*, 1981, **14**, 384–392.

12 D. M. Small, in *In Molecular Association in Biological and Related Systems*, American Chemical Society: Washington DC, 1968, vol. 84, ch. Size and Structure of Bile Salt Micelles, p. 31.

13 G. Esposito, E. Giglio, N. V. Pavel and A. Zanobi, *The Journal of Physical Chemistry*, 1987, **91**, 356–362.

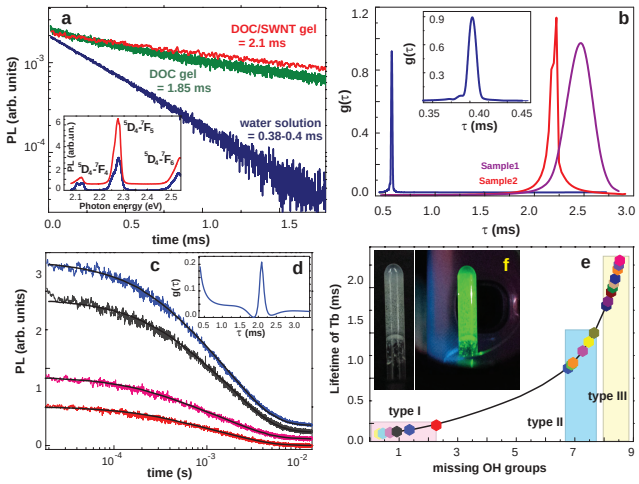

Fig. 1 (a) Semilogarithmic plot of the PL intensity versus time ($^5D_4 \rightarrow ^7F_5$ transition at 486 nm of excitation) for solvated Tb (blue), Tb encapsulated in DOC micelles confined in the pores of DOC-hydrogel (green) and in SWNT-DOC-hydrogel (red). Inset shows steady-state PL of Tb in water solution (blue) and SWNT-DOC-hydrogel (red). (b) Spectral distribution functions for $TbCl_3$ in DI water (blue), (magnified view in the inset), and in DOC/SWNT gel (red, purple). (c) Linear-log plot of the time-dependent PL of $^5D_4 \rightarrow ^7F_5$ (blue and black) and $^5D_4 \rightarrow ^7F_6$ (purple and red) transition in aged samples, at 486 nm of excitation (the curves are offset for clarity). (d) SDF for $^5D_4 \rightarrow ^7F_6$ line. (e) Correlation of the Tb lifetime and the number of missing OH-groups in the solvation shell with the content and morphology of Tb environment. (f) Typical Tb/DOC/SWNT hydrogel sample: image (left) and intense PL of $^5D_4 \rightarrow ^7F_5$ electronic transition at 488nm of excitation (right).

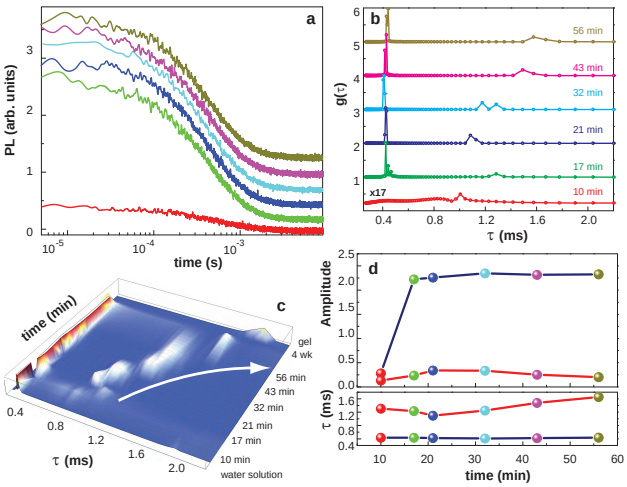

Fig. 2 Evolution of Tb-complexes upon diffusion into type II silica hydrogel: (a) Linear–log plot of the time-dependent PL of $^5D_4 \rightarrow ^7F_5$ transition in Tb at 488 nm of excitation (the curves are offset for clarity): color code is the same as in (b) and (d). Stretched-exponential shape is consistent with two lifetimes, τ_1 and τ_2. (b) Evolution of the spectral distribution function (SDF) during the time of experiment. (c) Comparison of SDF, peaked at corresponding lifetimes τ_1 ($\sim$0.4 ms) and τ_2 ($>$1 ms), for time duration of experiment and in the samples aged for several weeks. SDF of Tb in DI water (at the bottom of plot) and in type III DOC/SWNT gel (at the top) are added for completeness. (d) Lifetime and amplitude of the short- (blue) and long-lived (red) states of Tb for bi-exponential fit as a function of diffusion time.

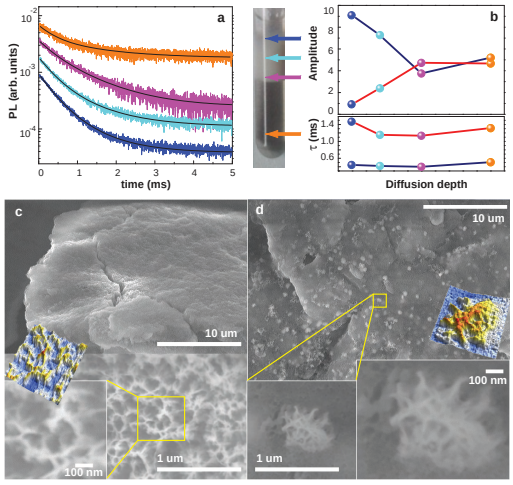

Fig. 3 Evolution of Tb-complexes upon diffusion into silica hydrogel taken 80 min after adding Tb on the top of the sample: (a) Semilogarithmic plot of the PL intensity versus time (same PL line as in Fig. 2, the curves are offset for clarity). The solid lines show bi-exponential fits obtained using Eq. (2); (b) corresponding lifetimes τ_1 (blue) and τ_2 (red), and amplitudes A_1 and A_2 for the states of Tb ions as a function of diffusion depth; (inset) PL loci (blue-cyan-pink-brown), top-to-bottom of the sample. (c,d) High-resolution SEM images show similar sub-micrometer structures both in (c) DOC gel formed from water solution and (d) DOC/SWNT silica hydrogel; insets show magnified views and false color 3D images of characteristic morphological features of DOC complexes.

14 A. A. D'Archivio, L. Galantini, E. Giglio and A. Jover, *Langmuir*, 1998, **14**, 4776–4781.

15 Z. Su, S. Luthra, J. F. Krzyzaniak, D. M. Agra-Kooijman, S. Kumar, S. R. Byrn and E. Y. Shalaev, *Journal of Pharmaceutical Sciences*, 2011, **100**, 4836–4844.

16 X. Sun, X. Xin, N. Tang, L. Guo, L. Wang and G. Xu, *The Journal of Physical Chemistry B*, 2014, **118**, 824–832.

17 W. Wenseleers, I. Vlasov, E. Goovaerts, E. Obraztsova, A. Lobach and A. Bouwen, *Advanced Functional Materials*, 2004, **14**, 1105–1112.

18 J. A. Fagan, M. Zheng, V. Rastogi, J. R. Simpson, C. Y. Khripin, C. A. Silvera Batista and A. R. Hight Walker, *ACS Nano*, 2013, **7**, 3373–3387.

19 E. H. Haroz, W. D. Rice, B. Y. Lu, S. Ghosh, R. H. Hauge, R. B. Weisman, S. K. Doorn and J. Kono, *ACS Nano*, 2010, **4**, 1955–1962.

20 Y. Liu, N. Zhang, Y. Chen and G.-S. Chen, *Bioorganic & Medicinal Chemistry*, 2006, **14**, 6615 – 6620.

21 S. M. Meyerhoffer and L. B. McGown, *Journal of the American Chemical Society*, 1991, **113**, 2146–2149.

22 A. Neves, A. Valente, H. Burrows, A. Ribeiro and V. Lobo, *Journal of Colloid and Interface Science*, 2007, **306**, 166 – 174.

23 J. G. Duque, C. G. Densmore and S. K. Doorn, *Journal of the American Chemical Society*, 2010, **132**, 16165–16175.

24 J. G. Duque, G. Gupta, L. Cognet, B. Lounis, S. K. Doorn and A. M. Dattelbaum, *The Journal of Physical Chemistry C*, 2011, **115**, 15147–15153.

25 G. Gupta, S. B. Rathod, K. W. Staggs, L. K. Ista, K. Abbou Oucherif, P. B. Atanassov, M. S. Tartis, G. A. Montao and G. P. Lpez, *Langmuir*, 2009, **25**, 13322–13327.

26 O. Moudam, B. C. Rowan, M. Alamiry, P. Richardson, B. S. Richards, A. C. Jones and N. Robertson, *Chem. Commun.*, 2009, 6649–6651.

27 P. R. Selvin and J. E. Hearst, *Proceedings of the National Academy of Sciences*, 1994, **91**, 10024–10028.

28 M. Xiao and P. R. Selvin, *Journal of the American Chemical Society*, 2001, **123**, 7067–7073.

29 M. Blades, T. Ignatova, J. G. Duque, S. K. Doorn and S. V. Rotkin, Bulletin of the APS March Meeting, 58 (1), Q1.00135, 2013.

30 T. Ignatova, M. Blades, J. G. Duque, S. K. Doorn and S. V. Rotkin, Proceedings of the 223rd Meeting of the Electrochemical Society; Toronto, Ontario, Canada; May 12-17, 2013, 2013.

31 D. C. Johnston, *Phys. Rev. B*, 2006, **74**, 184430.

32 M. Berberan-Santos, E. Bodunov and B. Valeur, *Chemical Physics*, 2005, **315**, 171 – 182.

33 A. Campanelli, S. Candeloro De Sanctis, E. Giglio, N. Viorel Pavel and C. Quagliata, *Journal of Inclusion Phenomena and Molecular Recognition in Chemistry*, 1989, **7**, 391–400.

34 M. Calabresi, P. Andreozzi and C. La Mesa, *Molecules*, 2007, **12**, 1731–1754.

35 H. Amenitsch, H. Edlund, A. Khan, E. Marques and C. L. Mesa, *Colloids and Surfaces A: Physicochemical and Engineering Aspects*, 2003, **213**, 79 – 92.

36 C. Liu and J. Hao, *The Journal of Physical Chemistry B*, 2011, **115**, 980–989.

37 M. H. V. Werts, R. T. F. Jukes and J. W. Verhoeven, *Phys. Chem. Chem. Phys.*, 2002, **4**, 1542–1548.